Applied Chemical Engineering (2025) Volume 8 Issue 3 ISSN: 2578-2010 (O)
doi: 10.59429/ace.v8i3.5735

ORIGINAL RESEARCH ARTICLE

Synergistic corrosion inhibition of carbon steel in cooling tower systems using sodium benzoate, zinc sulfate, and EDTA

Zahraa A. Jawad[1*], Falah K. Matloub[2]

12 University of Babylon, Chemical Engineering Department, Hilla, 51001, Iraq

***Corresponding author:** Zahraa A. Jawad; eng854.zahraa.abbas@student.uobabylon.edu.iq

ABSTRACT

The corrosion protection of cooling tower system is important due to the different types of salts and their concentrations increase continuously. The effectiveness of selected corrosion inhibitors—100 ppm sodium benzoate (C_6H_5COONa), 60 ppm zinc sulfate ($ZnSO_4$), and ethylenediaminetetraacetic acid (EDTA) at 10 and 20 ppm was investigated for carbon steel (CS) in saline environments with varying salt concentrations (1000, 3000, and 5000 ppm) and temperatures (28, 33, and 38 °C). Potentiodynamic polarization techniques were employed to assess corrosion potential (Ecorr), corrosion current density (Icorr), and Tafel slopes (βa and βc). The results demonstrated a significant reduction in corrosion rates with the addition of inhibitors. The highest inhibition efficiency, exceeding 96%, was achieved with 20 ppm EDTA at 33 °C in all salt concentrations. The synergistic effect of used inhibitors in mitigating corrosion was indicated. A notable synergistic effect among the inhibitors was also observed, further enhancing corrosion resistance.

Keywords: cathodic and anodic inhibitors; dispersant agent; blend of salts solution corrosion

ARTICLE INFO

Received: 17 August 2025
Accepted: 9 September 2025
Available online: 15 September 2025

1. Introduction

Corrosion represents one of the most significant hazards in contemporary industrial environments and heat exchangers, since it may rapidly deteriorate metals by oxidation and reduction through chemical and electrochemical processes [1,2]. Mild steel (MS) is extensively employed in industries for the construction of cooling tower systems owing to its low carbon content, durability, and cost-effectiveness.

Cooling towers are utilized as essential equipment to regulate temperature in any industrial processing machinery. It is very susceptible to corrosion due to the optimal conditions, which encompass a continuous flow of liquids containing dissolved salts, temperature, and various pH levels. [3]

The mitigation of corrosion primarily necessitates the regulation of the oxidation reaction (eq. 1) and reduction reaction (eq. 2) occurring on the metallic surface. The electrons produced in Reaction 1 are consumed in the second reaction (electroneutrality), resulting in both reactions transpiring simultaneously and at the same rate. These reactions can occur uniformly over the steel surface (microcells), resulting in either uniform corrosion or localized corrosion when particular cathodic and anodic sites are present on the metal. [4,5]

$$Fe \rightarrow Fe^{2+} + 2e^{-} \quad (1)$$

$$2H^+ + 2e^- \rightarrow H_2 \quad (2)$$

where reaction 1 is an anodic reaction (oxidation), and reaction 2 is a cathodic reaction (reduction).

Corrosion inhibitors are employed to safeguard metals against deterioration by creating protective barriers [6,7]. The compound must possess several properties to qualify as a certified corrosion inhibitor: it must be highly efficient, renewable, biodegradable, non-toxic, abundant in its components, suitable for the medium, stable at elevated temperatures, resistant to foaming or emulsification, and effective across various climatic conditions. [8,9]

Immersion corrosion inhibitors are liquid-phase inhibitors, including a group of different types that could be classified as cathodic or anodic inhibitors. The high corrosion rate in cooling tower system is due to the effect of increasing salt concentration, temperature variation, microbiological effect and galvanic corrosion of different metals and alloys, so synergistic inhibition approaches were used, to improve the corrosion resistance of cooling towers system [10,11]. The term "synergistic inhibition" describes the combined and intensified action of many corrosion inhibitors, which provide more protection than a single inhibitor.

Minerals that were formerly dissolved in water and then deposited onto heat transfer surfaces or in-flow water pipes are what cause scale to develop. In a cooling tower, the concentration of dissolved particles increases with water evaporation until it surpasses the solubility of a certain mineral salt that causes scale, particularly on heat exchanger transfer surfaces. Minerals caused scaling are silica, calcium sulphate ($CaSO_4$), calcium phosphate ($Ca_3(PO_4)_2$), and calcium carbonate ($CaCO_3$), typically in that order. Magnesium silicate scale may also form. While most calcium and magnesium salts are more soluble in cold water than in hot water, reverse trend of solubility of the majority of other salts [12,13]. The synergist inhibitors used in this research are anodic inhibitor (sodium benzoate), cathodic inhibitor (zinc sulfate) and scale dispersant (EDTA). The anodic and cathodic inhibitors have a combined effect for lowering corrosion rate while EDTA (as a dispersant) prevent the deposition of calcium and magnesium salts due to temperature increasing in heat exchangers.

The selected inhibitors sodium benzoate, zinc sulfate, and EDTA are industrially available and cost-effective, making them practical for use in open-loop cooling systems. However, each compound carries specific environmental and regulatory considerations. Sodium benzoate is generally recognized as safe and biodegradable, posing minimal environmental risk. Zinc sulfate, while effective as a cathodic inhibitor, can introduce ecotoxicity to aquatic organisms if discharged in high concentrations, and is subject to regulation under various environmental frameworks. EDTA, despite its efficacy in complexation and dispersion, is known for its environmental persistence and poor biodegradability, and may facilitate the transport of heavy metals in aquatic ecosystems. Therefore, the long-term industrial use of these inhibitors should be balanced with proper wastewater treatment and regulatory compliance.[14].

Mohammed et al. (2009) evaluated the corrosion inhibition performance of sodium benzoate and sodium nitrate on low-carbon steel in a 3% NaCl solution. Using potentiodynamic polarization they found that the highest inhibition efficiencies were 77% for sodium nitrate at 200 ppm and 74% for sodium benzoate at 5000 ppm. The polarization results, confirming the formation of a protective layer on the steel surface. The study concluded that both inhibitors are effective, with sodium nitrate showing slightly better performance under the tested conditions. [15]

Raheem et al. (2011) Carbon steel specimens immersed in a mixture of sodium phosphate ($Na_2\ HPO_4$), serving as a corrosion inhibitor, and sodium gluconate ($C_6H_{11}\ NaO_7$), acting as a scale dispersant, at different concentrations (20, 40, 60, 80 ppm) and temperatures (25, 50, 75, and 100 ºC) over a period of 1 to 5 days were examined. The effectiveness of the corrosion inhibitors was determined using unfettered and inhibited water, yielding a result of 98.1%. The findings of these research suggest that the corrosion rate decreases with an increase in the concentration of corrosion inhibitors at 80 ppm and at 100ºC during a duration of 5 days (i.e., corrosion rate = 0.014 gmd). of [16] Shaban et al. (2017) studied the combined effect of Sodium Benzoate and

EDTA as corrosion inhibitors for carbon steel in chloride-containing solutions, similar to those in cooling tower systems. They used electrochemical methods, including potentiodynamic polarization measure corrosion rates and inhibitor effectiveness .The results showed that using both inhibitors together gave a synergistic effect, with inhibition efficiency over 90%, much higher than using either one alone. The data indicated the formation of a strong protective layer on the steel surface, which reduced corrosion significantly. [17]

Brixi, et al. (2018) This study investigates the combined effects of EDTA and sodium benzoate on protecting mild steel from corrosion in a 3 % NaCl environment at various temperatures (25–55 °C). Using electrochemical impedance spectroscopy (EIS) and polarization techniques, the authors evaluated how temperature influences inhibitor performance.[18]

Ahmed et al.(2020) The corrosion of low carbon steel under the examined conditions demonstrated a noteworthy outcome, particularly with the NaCl percentage content. Initially, the corrosion rate escalated with a rise in salt content to 3.5%, reaching four times that of 0%; however, above this key threshold (3.5%), the corrosion rate decreased, ultimately falling below that of pure water. Increasing the solution flow rate to 2.5 l/min and the temperature to 50^{O}C will elevate the corrosion rate by 25% and 20%, respectively. The findings clearly indicate that a high concentration (>10%) of NaCl greatly inhibits the corrosion rate of mild steel, hence facilitating the use of saline in place of fresh water without reservation.[19]

Handi et al . (2022) Two distinct inhibitors, sodium molybdate and zinc phosphonate, were examined both separately and in combination at varying doses. Sodium molybdate (Na_2MoO_4) is a non-toxic anodic corrosion inhibitor, whereas zinc phosphonate serves as a cathodic inhibitor, both of which are environmentally safe. The optimal inhibitor concentrations were 4000 ppm for sodium molybdate and 20 ppm for zinc-phosphonate. The optimal inhibitor efficacy on the mild steel surface was attained with 50 ppm Zn-phosphonate combined with 300 ppm sodium molybdate, resulting in a 96% efficiency. [20]

Arief, et al. (2023) The efficacy and elucidating the mechanism of tannin and silica inhibitors, as well as the impact of including potassium iodide as a synergistic inhibitor were investigated. Utilising carbon steel samples immersed in demineralised water at temperatures ranging from 30 to 60°C for durations of 1, 2, and 3 hours. The concentration variations of tannins and silica used range from 0 to 1250 ppm. The findings indicated that the addition of potassium iodide was effective. The corrosion rate of mild steel decreased by 82.95% at a concentration of tannin-silica-KI at 1250 ppm. [21]

Author	Inhibitors Tested	Experimental Conditions	Inhibition Efficiency (%)	Notes / Novelty of Previous Study	Your Study Results	Novelty of Your Study (Highlights)
Mohammed et al. (2009)	Sodium benzoate, sodium nitrate	3% NaCl, potentiodynamic polarization	77% (NaNO3 at 200 ppm), 74% (Na-benzoate at 5000 ppm)	Confirmed protective film formation; high concentration required	Combination of inhibitors at lower concentrations achieved high efficiency	Achieved high inhibition at lower inhibitor concentrations
Raheem et al. (2011)	Sodium phosphate & sodium gluconate	20-80 ppm, 25-100 °C, 1-5 days	Up to 98.1% at 80 ppm and 100 °C	Studied temperature and concentration effects on inhibition	Evaluated effects of multiple saline concentrations and temperatures	Realistic operating conditions with environmental and practical relevance
Shaban et al. (2017)	Sodium benzoate + EDTA (combined)	Chloride solutions, electrochemical methods	>90% synergistic effect	Synergistic inhibition demonstrated	Synergistic effects analyzed with different inhibitor combinations	Detailed mechanism and enhanced performance

						with novel mixtures
Brixi et al. (2018)	EDTA + sodium benzoate	3% NaCl, 25-55 °C, EIS & polarization	Not specified	Investigated temperature influence via electrochemical impedance spectroscopy	Applied advanced techniques to evaluate temperature impact	Extended knowledge on temperature effects on inhibitor performance
Ahmed et al. (2020)	NaCl concentration effect only	Varied NaCl %, flow rate, 50 °C	Not specified	Corrosion rate peaked at 3.5% NaCl then decreased	Combined saline concentration and temperature effects with inhibitors	Multi-variable approach in realistic operational environments
Handi et al. (2022)	Sodium molybdate, zinc phosphonate	Various doses, low-carbon steel	96% (combo of 50 ppm Zn-phosphonate + 300 ppm Mo)	Environmentally safe inhibitors with synergistic effect	Environmentally friendly inhibitors combined with traditional ones	Emphasis on eco-friendly inhibitors with high efficiency
Arief et al. (2023)	Tannin, silica, potassium iodide	Demineralized water, 30-60 °C, up to 1250 ppm	82.95% (tannin-silica-KI at 1250 ppm)	Clear synergistic effect using natural inhibitors	Use of natural organic inhibitors with new synergistic additives	Use of natural, eco-friendly inhibitors with improved synergy
Your Study	Sodium benzoate (100 ppm), zinc sulfate (60 ppm), EDTA (10 & 20 ppm)	Various saline concentrations (1000, 3000, 5000 ppm), temperatures (28, 33, 38 °C)	>96% (20 ppm EDTA at 33 °C)	Investigated synergy and varied saline concentration/temperature	Highest efficiency (>96%) at lower concentrations with synergy effect	Achieved high inhibition at low concentrations with practical temp/salinity ranges; comprehensive synergy study

2. Experimental work

2.1. Chemical composition of low carbon steel pieces

Table 1. Chemical composition of carbon steel pieces

Element	Mn	Si	P	S	Cr	Ni	W	V	Mo	Al	Ti	Cu	As
Content %	3.867	2.222	0.001	0	1.12	18.297	0.021	0	1.116	0.775	0.748	0.763	0.000

2.2. Working electrode preparation

Cylindrical samples of carbon steel (CS) about 2.3 cm in length and 5 mm diameter were used and a suitable length of copper wire was welded to one end. The steel specimens are covered by epoxy resin to prevent contact with the corrosive media. The cross-sectional area of each specimen equals 0.1964 cm^2 as shown in **Figure 1** and **2**. The surface of the sample was polished to remove trace of contaminants, then degreased using alcohol. This was carried out to improve the adhesion of the epoxy mounting resin to the metal and reduce the tendency to crevice corrosion at the edge of the mounting resin. The exposed surface of the test specimens was initially prepared by polishing using a series of successively finer grades of silicon carbide abrasive papers (200,400 and 600 grade) under running water. The polished specimen washed with distilled water and dried by tissue paper then washing with ethanol and dried by tissue paper and finally stored in desiccator on silica gel.

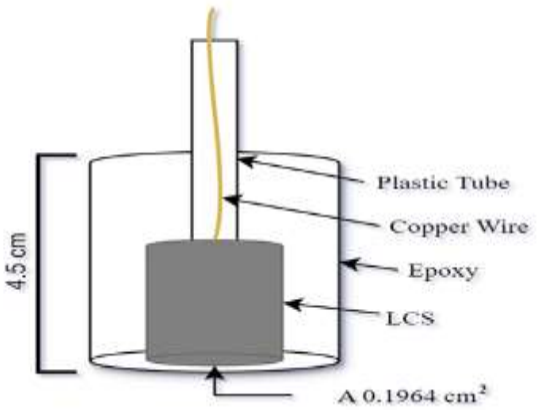

Figure 1. Schematic diagram for the working electrode

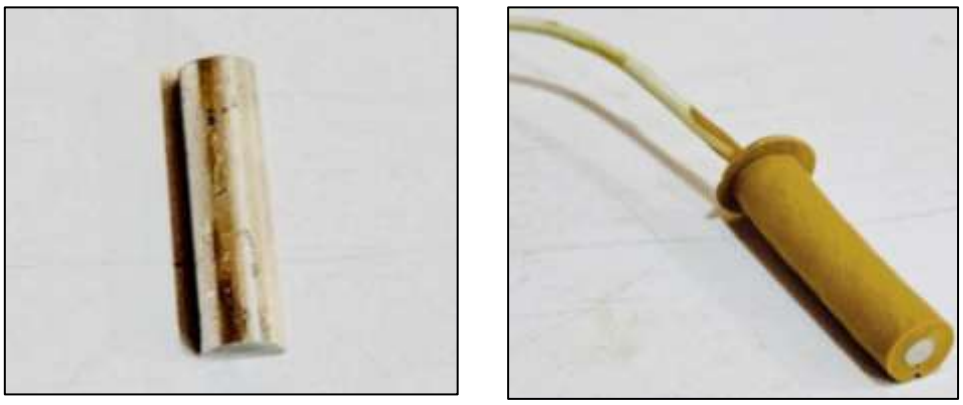

(A) (B)

Figure 2. The specimen (A) before coating with epoxy , (B) coated working electrode

3. Preparation of the electrolyte

Electrolyte solutions were prepared at three different total salt concentrations: 1000 ppm**,** 3000 ppm, and 5000 ppm, in order to simulate varying salinity levels commonly found in environmental and industrial water systems. These concentrations were carefully selected to represent realistic conditions that could influence the physical and chemical behavior of water.

The 5000 ppm solution was prepared using local tap water and analytical-grade salts, as detailed in **Table 2**. The 1000 ppm and 3000 ppm solutions were subsequently obtained by diluting the 5000 ppm solution with deionized water, to avoid introducing any additional ions or impurities that might affect the chemical composition or behavior of the solution.

For the preparation process, the required amounts of each salt were accurately weighed using a precision balance. The salts were then gradually added to a 1-liter flask containing approximately 800 mL of water (either distilled or tap water). The solution was stirred thoroughly using a glass rod to ensure complete dissolution of all components. After full dissolution was achieved, the volume was brought up to 1 liter by adding the appropriate amount of water.

The pH of the solution was measured using a calibrated pH meter, and the values were found to range between 8.0 and 8.5. This slightly alkaline range is attributed to the presence of basic salts such as calcium carbonate and sodium-based compounds in the solution.

Table 2. concentration of different salts presence in water .

Concentration ppm	*NaCl*	*Na_2SO_4*	*$MgCl_2$*	*$CaCl_2$*	*$CaCO_3$*	*tap Water*
5000 ppm	1600 ppm	1000 ppm	500 ppm	600 ppm	750 ppm	550 ppm

4. Inhibitor concentrations

The concentration of inhibitors (Sodium Benzoate (C_6H_5CooNa), Zinc Sulphate ($ZnSO_4$) and Ethylenediaminetetraacetic acid (EDTA)) are shown in (**Table 3**).

Table 3. The types and concentrations of inhibitors.

Type of inhibitor	**Concentration *ppm***
C_6H_5COONa	*100 ppm*
$ZnSO_4$	60 ppm
EDTA	10 ppm and 20 ppm

5. Polarization technique

Polarization assessments were performed via a multichannel potentiostat (MLab 200). A standard calomel electrode (SCE) served as the reference electrode, while graphite functioned as the auxiliary electrode, alongside the CS as the working electrode. The distance between the working and reference electrodes was maintained at about (1-2) mm. The efficiency of inhibition was determined using equation 3 and the electrochemical corrosion testing diagram shown in **Figure 3**.

$$\eta\% = \frac{i^{\circ}corr - i^{i}corr}{i^{\circ}corr} \times 100\% \quad (3)$$

where:

$i^{\circ}corr$= corrosion current without inhibitor,

$i^{i}corr$ = corrosion current with inhibitor.

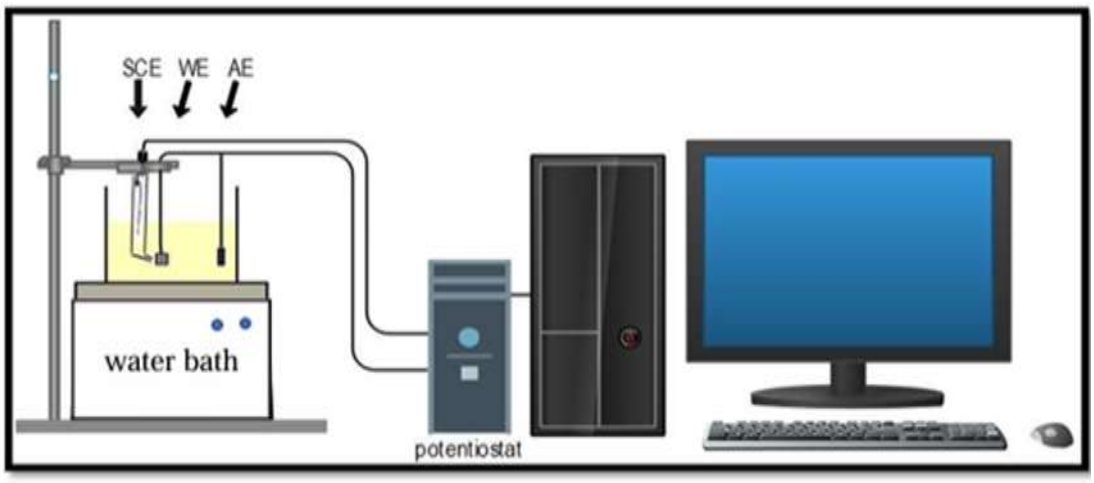

Figure 3. Electrochemical potentiodynamic polarization

6. Results and discussion

The results of all experiments are listed and represented in the following tables and figures.

Table 4. corrosion current, E_{corr}, I_{corr} and tafel constants in different salts concentration without inhibitors at 28 C°

Run	Conc.(ppm)	E_{corr} (mV)	I_{corr}.(µA)	βc mV/dec^{-1}	βa mV/dec^{-1}	η%
1	1000	-768	0.531	-96.9	81.2	-
2	3000	-778	0.611	-153.9	132.1	-
3	5000	-690	0.706	-71.0	37.3	-

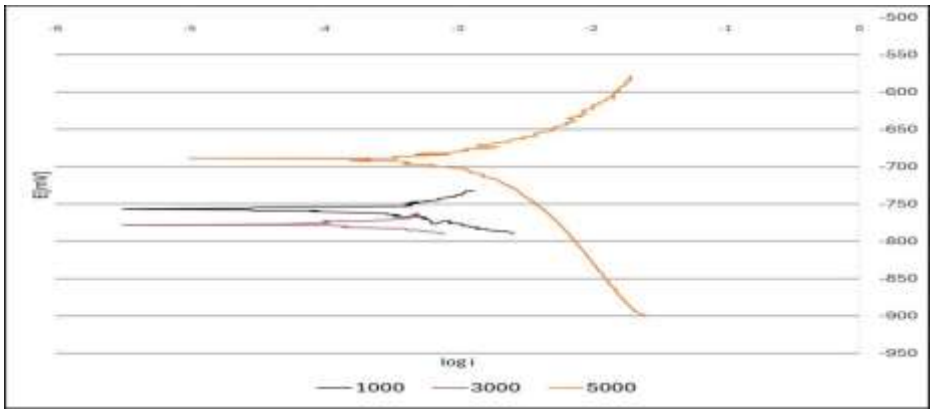

Figure 4. Potentiodynamic polarization curves for (CS) samples in various concentrations without inhibitor at 28°C

Table 5. corrosion current, E_{corr}, I_{corr}, tafel constants and efficiency at different salts concentration and 100ppm sodium benzoate, 60ppm zinc sulfate and without EDTA at 28C°

Run	Conc.(ppm)	E_{corr}. (mV)	I_{corr}.(µA)	βc mV/dec^{-1}	βa mV/dec^{-1}	η%
1	1000	-631	0.356	-97.5	123.2	32.9
2	3000	-754	0.382	-94.1	101.9	37.4
3	5000	-687	0.462	-82.4	67.8	34.5

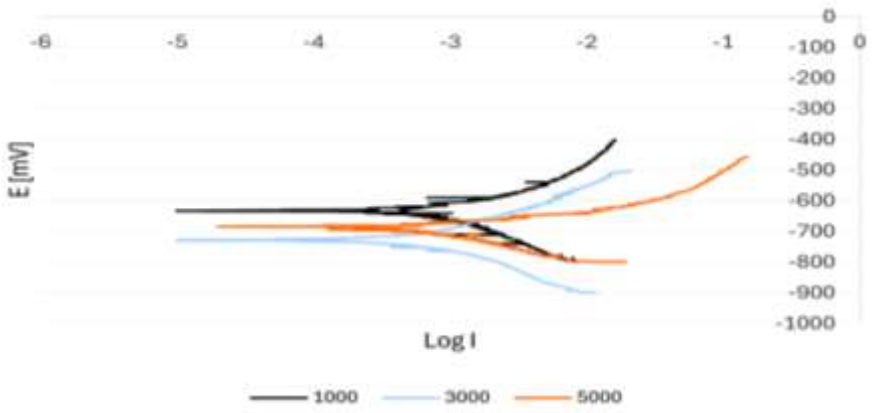

Figure 5. Potentiodynamic polarization curves for (CS) samples in various concentrations of C_6H_5CooNa 100 ppm, $ZnSO_4$ 60 ppm without EDTA at 28°C

Table 6. Corrosion current, E_{corr}, I_{corr}, tafel constants and efficiency at different salts concentration and 100ppm sodium benzoate, 60ppm zinc sulfate and 10 ppm EDTA at 28C°

Run	Conc.(ppm)	E_{corr}. (mV)	I_{corr}.(µA)	βc mV/dec^{-1}	βa mV/dec^{-1}	η%
1	1000	-1021	0.110	-83.1	105.8	79.2
2	3000	-894	0.214	-42.0	79.2	64.9
3	5000	-949	0.341	-75.5	153.1	51.6

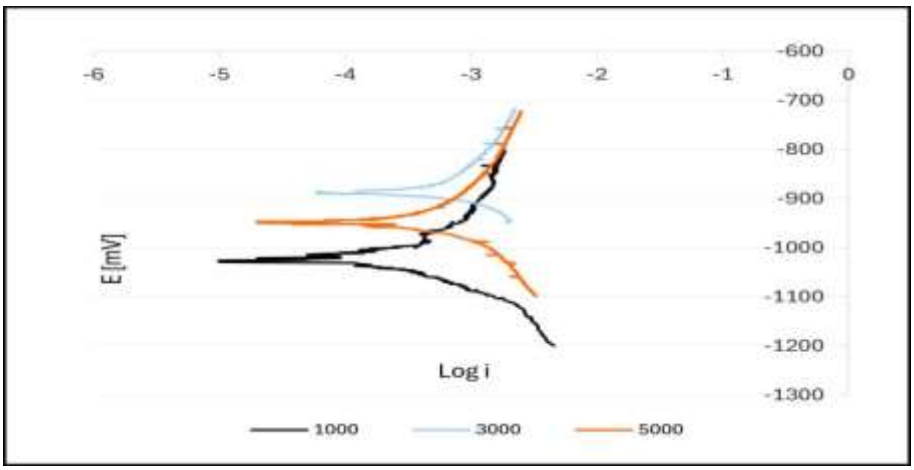

Figure 6. Potentiodynamic polarization curves for (CS)samples in various concentrations of C_6H_5CooNa 100 ppm and $ZnSO_4$ 60 ppm with 10 ppm EDTA and at 28°C

Table 7. corrosion current, E_{corr}, I_{corr}, tafel constants and efficiency at different salts concentration and 100ppm sodium benzoate, 60ppm zinc sulfate and 20 ppm EDTA at 28C°

Run	Conc.(ppm)	$E_{corr.}$ (mV)	$I_{corr.}$(µA)	βc mV/dec^{-1}	βa mV/dec^{-1}	η%
1	1000	-876	0.0329	-63.1	110.8	93.8
2	3000	-988	0.0341	-48.4	116.5	94.4
3	5000	-836	0.0437	-66.7	72.2	93.2

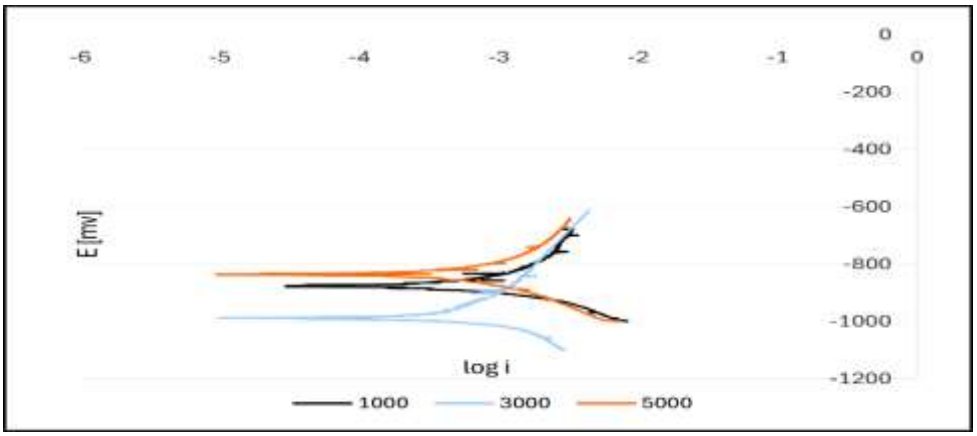

Figure 7. Potentiodynamic polarization curves for (CS) samples in various concentrations of C_6H_5CooNa 100 ppm and $ZnSO_4$ 60 ppm with 20 ppm EDTA and at 28°C

Table 8. corrosion current, E_{corr}, I_{corr} and tafel constants at different salts concentration without inhibitor at 33 C°

Run	Conc.(ppm)	E_{corr}(mV)	$I_{corr.}$(µA)	βc mV/dec^{-1}	βa mV/dec^{-1}	η%
1	1000	-548	2.8	-77.6	75.1	-
2	3000	-581	3.06	-92.4	84.2	-
3	5000	-591	4.5	-105.7	96.8	-

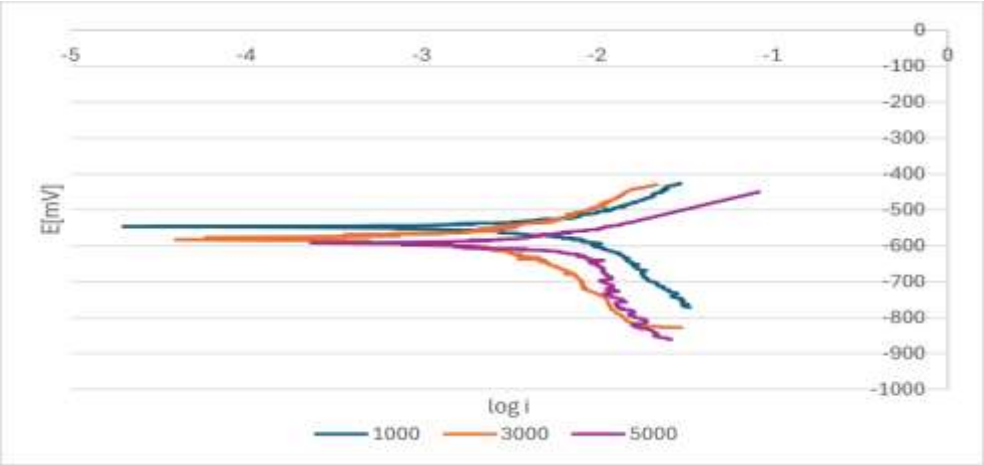

Figure 8. Potentiodynamic polarization curves for (CS) samples in various concentrations without inhibitor at 33C°

Table 9. corrosion current, E_{corr}, I_{corr}, tafel constants and efficiency at different salts concentration and 100ppm sodium benzoate, 60ppm zinc sulfate and without EDTA at temperature 33C°.

Run	Conc.(ppm)	E_{corr}(mV)	$I_{corr.}$(µA)	βc mV/dec^{-1}	βa mV/dec^{-1}	η%
1	1000	-669	0.552	-86.4	69.0	80.2
2	3000	-642	0.620	-100.2	56.2	79.7
3	5000	-705	0.741	-71.5	83.5	84.1

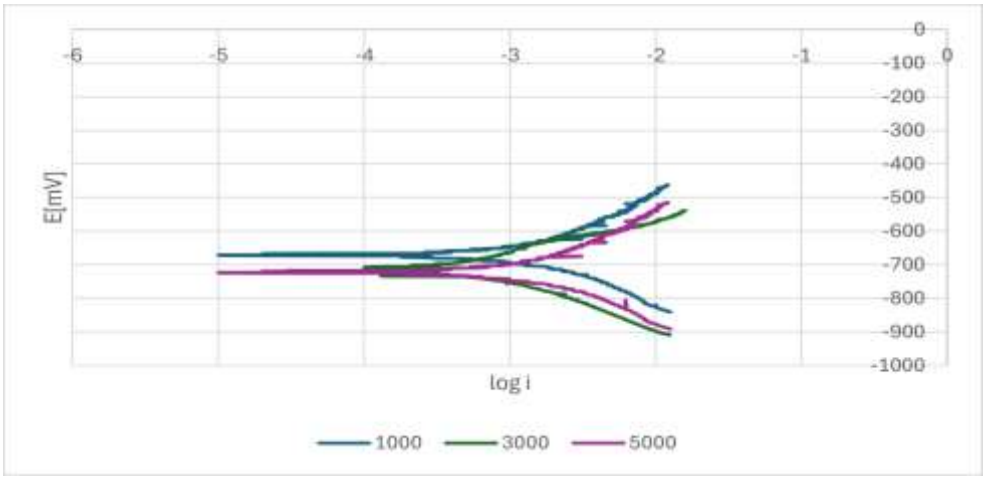

Figure 9. Potentiodynamic polarization curves for (CS) samples in various concentrations of C_6H_5COONa 100 ppm, $ZnSO_4$ 60 ppm at 33C°

Table 10. corrosion current, E_{corr}, I_{corr}, tafel constants and efficiency at different salts concentration and 100ppm sodium benzoate, 60ppm zinc sulfate and 10ppm EDTA at 33C°.

Run	Conc.(ppm)	$E_{corr.}$(mV)	$I_{corr.}$(µA)	βc mV/dec^{-1}	βa mV/dec^{-1}	η%
1	1000	-627	0.176	-100.1	68.4	93.7
2	3000	-634	0.296	-67.4	61.1	90.3
3	5000	-655	0.400	-86.0	75.2	91.1

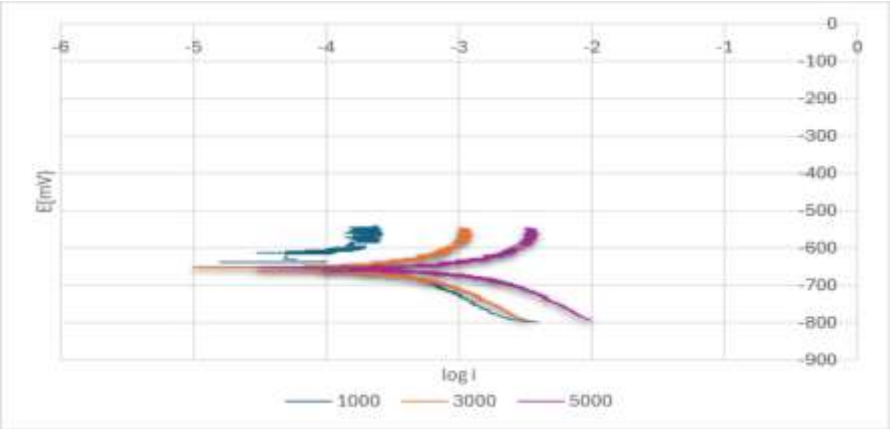

Figure 10. Potentiodynamic polarization curves for (CS) samples in various concentrations of C_6H_5CooNa 100 ppm and $ZnSO_4$ 60 ppm with 10 ppm EDTA at 33C°

Table 11. corrosion current, E_{corr}, I_{corr}, tafel constants and efficiency at different salts concentration and 100 ppm sodium benzoate, 60ppm zinc sulfate and 20 ppm EDTA at 33C°.

Run	Conc.(ppm)	$E_{corr.}$(mv)	$I_{corr.}$(µA)	βc mV/dec^{-1}	βa mV/dec^{-1}	η%
1	1000	-643	0.0352	-72.3	86.4	98.7
2	3000	-505	0.0573	-123.2	93.5	98.1
3	5000	-610	0.075	-62.0	56.8	98.3

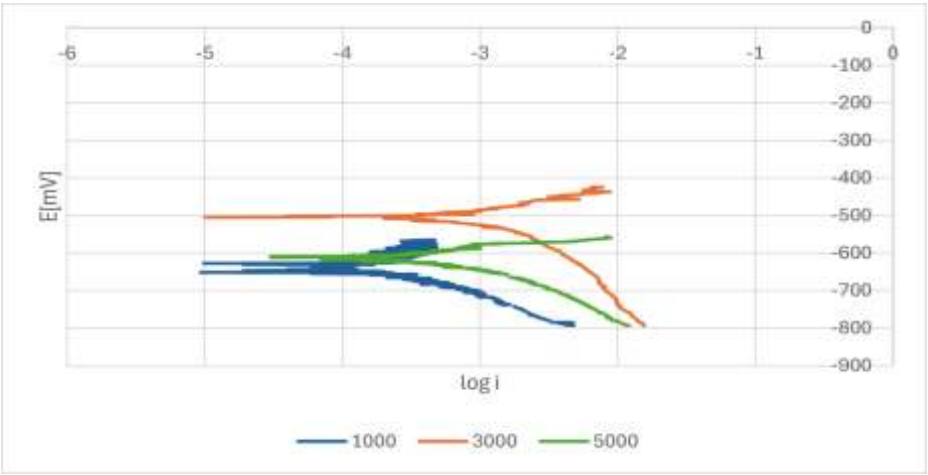

Figure 11. Potentiodynamic polarization curves for (CS) samples in various concentrations of C_6H_5CooNa 100 ppm and $ZnSO_4$ 60 ppm with 20 ppm EDTA at 33C°

Table 12. Corrosion current ,E_{corr} I_{corr}, and tafel constants at different salts concentration without inhibitor at 38 C° .

Run	Conc.(ppm)	$E_{corr.}$ (mV)	$I_{corr.}$(µA)	βc mV/dec^{-1}	βa mV/dec^{-1}	η%
1	1000	-1137	3.52	-60.6	52.9	-
2	3000	-1061	4.20	-71.9	57.8	-
3	5000	-1136	5.21	-67.2	78.4	-

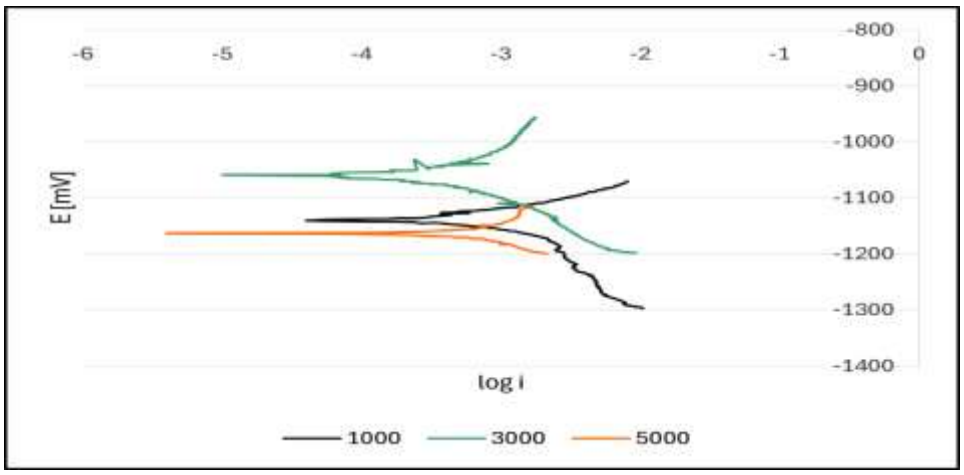

Figure 12. Potentiodynamic polarization curves for (CS) samples in various concentrations at 38°C without inhibitor

Table 13. Corrosion current, E_{corr}, I_{corr}, tafel constants and efficiency at different salts concentration and 100ppm sodium benzoate, 60ppm zinc sulfate and without EDTA at 38C°.

Run	Conc.(ppm)	$E_{corr.}$ (mV)	$I_{corr.}$(µA)	βc mV/dec^{-1}	βa mV/dec^{-1}	η%
1	1000	-576	0.666	-96.8	132.1	81.2
2	3000	-589	0.876	-53.2	30.6	79.1
3	5000	-680	0.992	-44.7	203.7	80.9

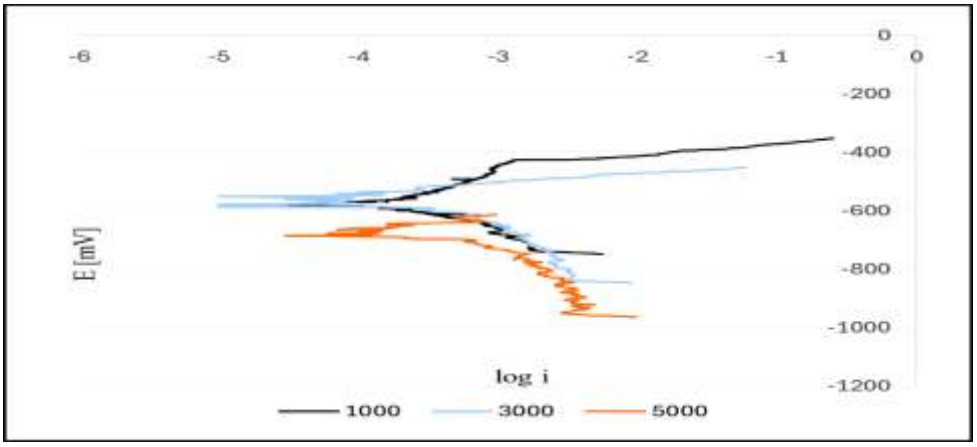

Figure 13. Potentiodynamic polarization curves for (CS) samples in various concentrations of C_6H_5CooNa 100 ppm and $ZnSO_4$ 60 ppm and at 38°C

Table 14. Corrosion current,E_{corr}, I_{corr} ,tafel constants and efficiency at different salts concentration and 100ppm sodium benzoate, 60ppm zinc sulfate and 10 ppm EDTA at 38C°.

Run	Conc.(ppm)	$E_{corr.}$ (mV)	$I_{corr.}$(µA)	βc mV/dec^{-1}	βa mV/dec^{-1}	η%
1	1000	-1154	0.253	-87.1	105.1	92.8
2	3000	-1161	0.374	-69.9	46.3	91.1
3	5000	-1163	0.530	-111.8	84.3	89.8

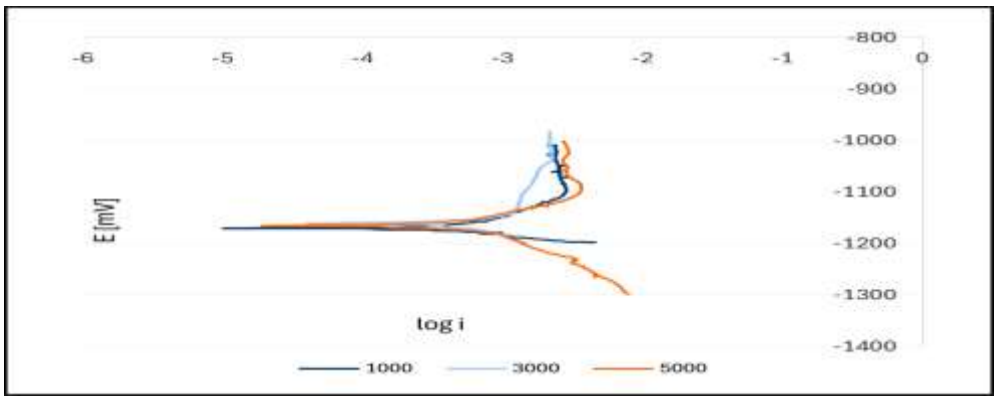

Figure 14. Potentiodynamic polarization curves for (CS) samples in various concentrations of C_6H_5CooNa 100 ppm and $ZnSO_4$ 60 ppm with 10 ppm EDTA and at 38°C

Table 15. Corrosion current,E_{corr}, I_{corr}, tafel constants and efficiency at different salts concentration and 100ppm sodium benzoate, 60ppm zinc sulfate and 20 ppm EDTA at 38C°.

Run	Conc.(ppm)	$E_{corr.}$ (mV)	$I_{corr.}$(µA)	βc mV/dec^{-1}	βa mV/dec^{-1}	η%
1	1000	-1137	0.0977	-79.1	52.1	97.2
2	3000	-872	0.156	-47.6	64.7	96.3
3	5000	-920	0.192	-84.9	58.6	95.3

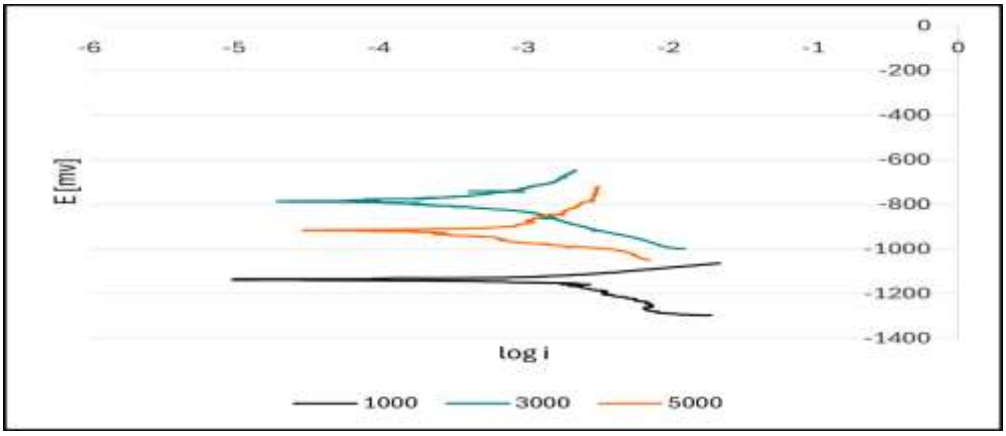

Figure 15. Potentiodynamic polarization curves for (CS) samples in various concentrations of C_6H_5CooNa 100 ppm and $ZnSO_4$ 60 ppm with 20 ppm EDTA and at 38°C

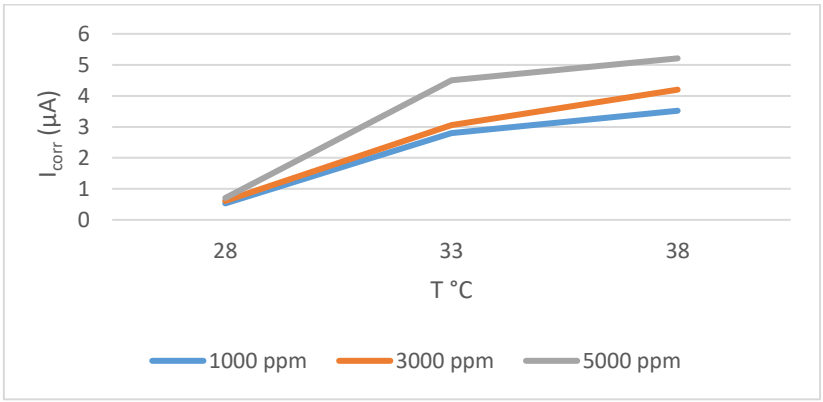

Figure 16. Effect of temperatures on corrosion rate for (CS) samples in different concentrations without inhibitor

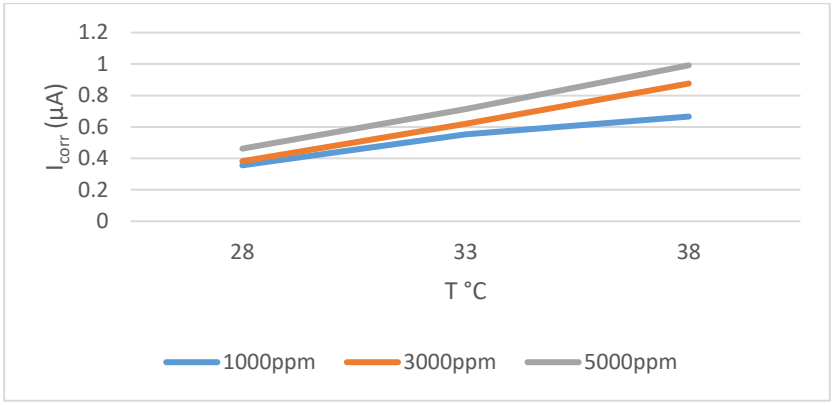

Figure 17. Effect of temperatures on corrosion rate for (CS) samples in different concentration with inhibitor of(C6H5CooNa 100 ppm and ZnSO4 60 ppm)

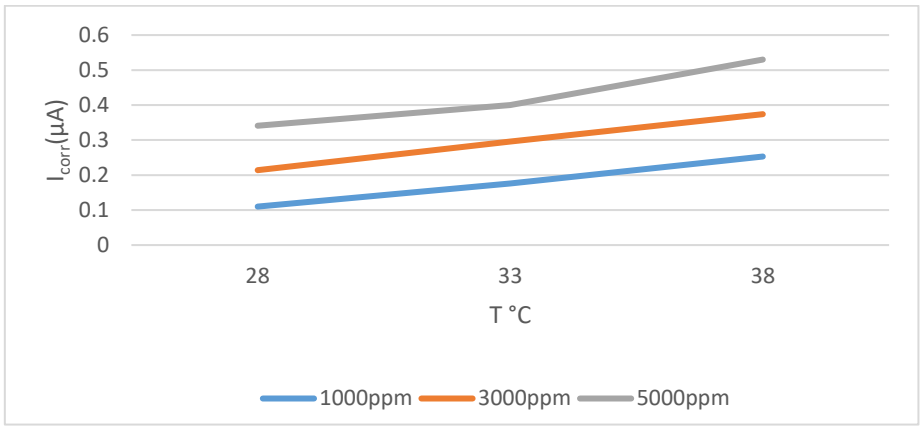

Figure 18. Effect of temperatures on corrosion rate for (CS) samples in different concentration with in inhibitor of(C6H5CooNa 100 ppm and ZnSO4 60 ppm) with 10 ppm EDTA

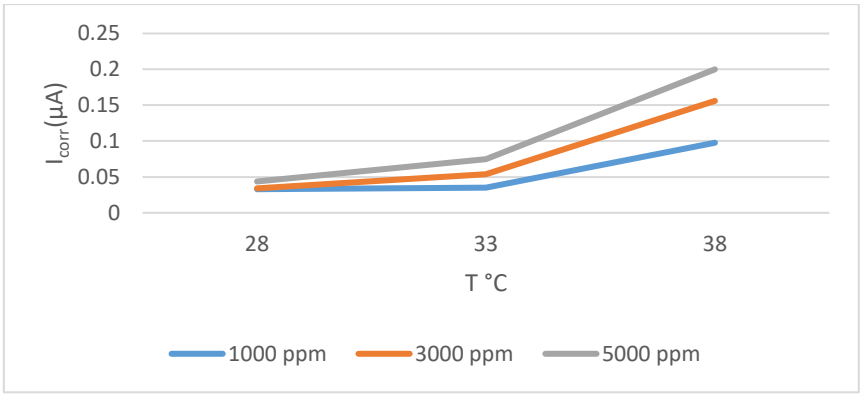

Figure 19. Effect of temperatures on corrosion rate for (CS) samples in different concentration with in inhibitor of(C6H5CooNa 100 ppm and ZnSO4 60 ppm) with 20 ppm EDTA

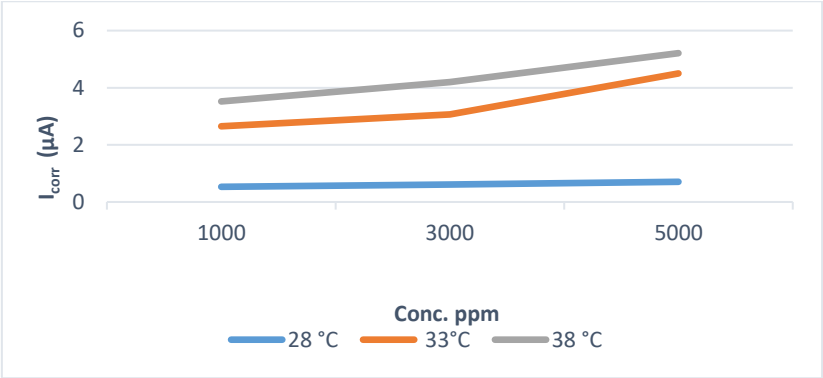

Figure 20. Effect of concentration on corrosion rate for (CS) samples in different temperatures without inhibitor

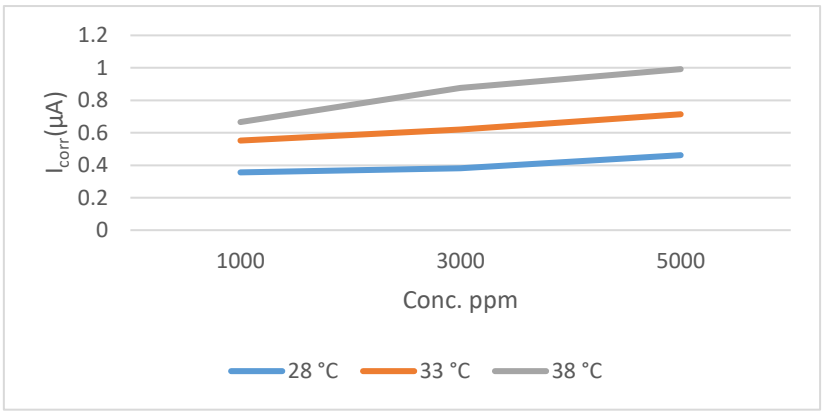

Figure 21. Effect of concentration on corrosion rate for (CS) samples in different temperatures with inhibitor of(C6H5CooNa 100 ppm and ZnSO4 60 ppm)

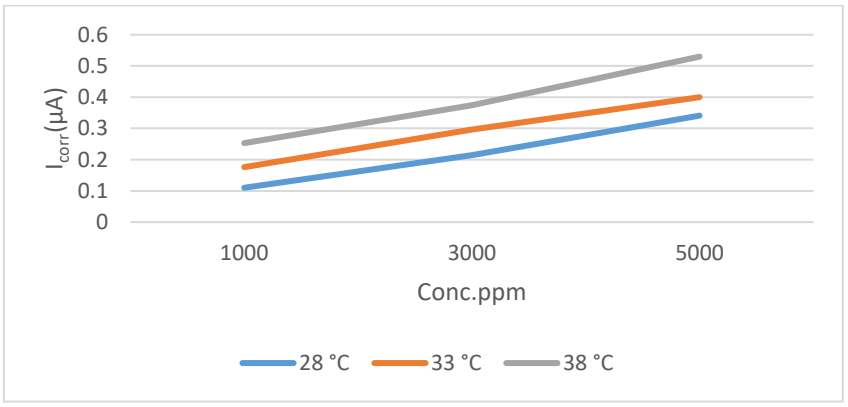

Figure 22. Effect of concentration on corrosion rate for (CS) samples in different temperatures with inhibitor of(C6H5CooNa 100 ppm and ZnSO4 60 ppm) with 10 ppm EDTA

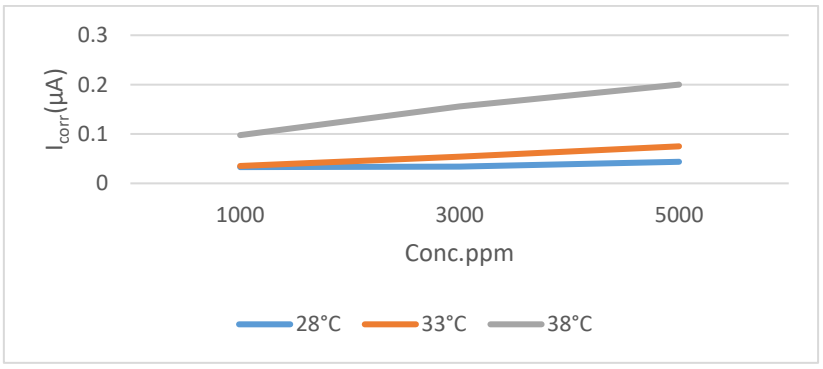

Figure 23. Effect of concentration on corrosion rate for (CS) samples in different temperatures with inhibitor of (C6H5COONa 100 ppm and ZnSO4 60 ppm) with 20 ppm EDTA

The study investigated the corrosion behavior of carbon steel (CS) in different salt concentrations (1000, 3000 and 5000 ppm) at different temperatures (28°C, 33°C, and 38°C), both in the absence and presence of corrosion inhibitors (sodium benzoate (100 ppm), zinc sulfate (60 ppm), and EDTA (scale dispersant) (10 ppm and 20 ppm)).

The corrosion current density ($\mathbf{I_{corr}}$) increases with increasing salt concentration and temperature in the absence of inhibitors. This is expected, as ions concentrations increase the conductivity of the solution increase and the transfer of ions increase. If the temperature increases the activity and mobility of the metal molecules will increase and viscosity of the solution will decrease, so the possibility of attack increases. Active ions like halogens may penetrate passive films, it means destroying the passive film and preventing passivity due to corrosion process. Generally, the elevated temperatures enhance the electrochemical activity of the metal and solution constituents which accelerate the corrosion process (corrosion rate). The increase in temperature from 28°C to 38°C led to a noticeable rise in $\mathbf{I_{corr}}$ values, indicating that corrosion becomes more active at higher temperatures—an expected outcome due to the accelerated rate of electrochemical reactions. For instance, at 28°C I_{corr} increased from **0**.531 µA (1000 ppm) to 0.706 µA (5000 ppm). Similarly, at 33°C I_{corr} rose from 2.8 µA (1000 ppm) to 4.5 µA (5000 ppm). and, for 38 °C I_{corr} growing from 3.52 µA (1000 ppm) to 5.21 µA (5000 ppm).

The introduction of sodium benzoate and zinc sulfate significantly reduced I_{corr} at all temperatures, indicating effective inhibition. For example, at 33°C and 5000 ppm salt (figure 6), I_{corr} decreased from 4.5 µA (no inhibitor) to 0.992 µA, with an inhibition efficiency (η%) of 77.9**%**. The reduction is due to the adsorption of inhibitor molecules on the metal surface, forming a protective barrier against corrosion. However, inhibition efficiency varied with salt concentration, with a slight decrease at higher concentrations, likely due to competitive adsorption between salt ions and inhibitor molecules

Adding EDTA to the inhibitors blend resulted in a remarkable improvement in corrosion inhibition. At 28°C, the blend with 10 ppm EDTA (**Figure 3**) showed high inhibition efficiency (up to 79.2%) This improvement in efficiency is not attributed to the direct adsorption of EDTA onto the metal surface, but rather to its ability to improve the electrochemical environment by chelating metal ions and preventing their harmful accumulation, which can otherwise promote localized corrosion or interfere with inhibitor performance. at 33°C. At this temperature, 10 ppm EDTA improved inhibition efficiency to over 96%, and 20 ppm EDTA further increased it up to 98.7% (**Figure 4.8**). This enhancement is likely due to the chelating properties of EDTA, which can form stable complexes with metal ions, reducing their participation in electrochemical reactions. Additionally, EDTA may improve the surface coverage of the other inhibitors, resulting in a more compact and stable protective film. The deposition of salts on the metal surface increases the possibility of corrosion occurring at a higher rate due to formation of covered spots and uncovered areas on the metal surface which create potential difference.

At 38°C, however, the effectiveness of the inhibitors decreased, particularly with 10 ppm EDTA (**Figure 4-11**), where η% dropped to 89.8% at 5000 ppm. This could be due to less adsorption of inhibitor molecules. Nonetheless, increasing EDTA to 20 ppm (**Figure 4-12**) helped recover efficiency to 95.5%, confirming that higher EDTA concentration partially compensates for higher adsorption of the inhibitor on the bare surface of the metal.

Figures 13-20 illustrate that the corrosion rate (corrosion current) increase with temperature and concentration of salts increasing and decreasing with addition inhibitors and EDTA.

The corrosion potential has no effect on corrosion measurement due to the dual effect of inhibitors (anodic and cathodic) which eliminate the rising of corrosion potential or lowering by other inhibitor. The tafel constants which measured by the polarization curve. The intersection of cathodic tafel constant with horizontal line passes through corrosion potential could be indicate to the corrosion current value.

7. Conclusion

Corrosion rate of CS increased with both salt concentration and temperature, as reflected by higher Icorr values in uninhibited systems.The binary inhibitor system (sodium benzoate + zinc sulfate) demonstrated moderate protection, with efficiencies up to 78%.Addition of EDTA at 10 ppm significantly improved inhibition efficiency, particularly at 33°C, due to its chelating action and facilitation of stable passive layer formation.The optimal performance is achieved at 20 ppm EDTA, where inhibition efficiencies exceeded 98%, indicating strong synergistic effects when all three components are present. The study highlights the importance of balancing inhibitor concentration, temperature, and salinity to achieve effective corrosion protection.

Conflict of interest

The authors declare no conflict of interest

References

1. Ismail, N. A., Moussa, A. M., Kahraman, R., & Shakoor, R. A. (2022). Study on the corrosion behavior of polymeric nanocomposite coatings containing halloysite nanotubes loaded with multicomponent inhibitor. Arabian Journal of Chemistry, 15(9), 104107. https://doi.org/10.1016/j.arabjc.2022.104107
2. Díaz-Jiménez, V., Gómez-Sánchez, G., Likhanova, N. V., Arellanes-Lozada, P., Olivares-Xometl, O., Lijanova, I. V., & Arriola-Morales, J. (2024). Current overview of corrosion inhibition of API steel in different environments. ACS Omega, 9(26), 27798–27831. https://doi.org/10.1021/acsomega.4c02108
3. El-Enin, S. A., and Amin, A. (2015). Review of corrosion inhibitors for industrial applications. International Journal of Engineering Research and Review, 3(2), 127–145.
4. Wagner, T. V., Parsons, J. R., Rijnaarts, H. H. M., de Voogt, P., and Langenhoff, A. A. M. (2018). A review on the removal of conditioning chemicals from cooling tower water in constructed wetlands. Critical Reviews in Environmental Science and Technology, 48, 1094–1125. https://doi.org/10.1080/10643389.2018.1512289
5. Li, C.-Q., and Yang, W. (2021). Steel corrosion and degradation of its mechanical properties. CRC Press.
6. Kokilaramani, S., Satheeshkumar, A., Nandini, M. S., Narenkumar, J., AlSalhi, M. S., Devanesan, S., ... & Malik, T. (2024). Application of photoelectrochemical oxidation of wastewater used in the cooling tower water and its influence on microbial corrosion. Frontiers in Microbiology, 15, 1297721.
7. Cherrad, S., Alrashdi, A. A., Lee, H. S., Elaoufir, Y., Lgaz, H., Satrani, B., Ghanmi, M., Aouane, E. M., and Chaouch, A. (2022). Cupressus arizonica fruit essential oil: A novel green inhibitor for acid corrosion of carbon steel. Arabian Journal of Chemistry, 15. https://doi.org/10.1016/j.arabjc.2022.103849
8. Grassino, A. N., Cindrić, I., and Halambek, J. (2021). Green corrosion inhibitors from biomass and natural sources. In Sustainable Corrosion Inhibitors (Vol. 107, p. 46). Elsevier.
9. Pourzarghan, V., & Fazeli-Nasab, B. (2021). The use of Robinia pseudoacacia L. fruit extract as a green corrosion inhibitor in the protection of copper-based objects. Heritage Science, 9(1), 1–14. https://doi.org/10.1186/s40494-021-00545-z
10. Davis, J. R. (2000). Corrosion: Understanding the basics. ASM International.
11. Roberge, P. R. (2019). Handbook of corrosion engineering (2nd ed.)McGraw-Hill Education.
12. Baboo, P. (2020). Integrated cooling tower for fertilizer complex: A new approach. International Journal of Engineering Research and Technology (IJERT, 9)(8), 1–10.
13. Liu, X., Wu, S., Qin, Y., Zhang, Y., Li, W., and Wang, Z. (2025). In-depth research into the synergistic inhibition mechanism of amino acids and KI on the corrosion of carbon steel in acidic medium. Journal of Solid State Electrochemistry. https://doi.org/10.1007/s10008-
14. Simate, G. S., Ndlovu, S., & Iyuke, S. E. (2017). A review of industrial cooling water treatment technologies and management practices. Journal of Cleaner Production, 168, 1075–1090. https://doi.org/10.1016/j.jclepro.2017.09.058
15. Mohammed, B. A., & Mohana, K. N. (2009). The effect of sodium benzoate and sodium nitrate on the corrosion behavior of low carbon steel in chloride medium. Monatshefte für Chemie - Chemical Monthly, 140(1), 1–8. https://doi.org/10.1007/s00706-008-0018-1
16. Raheem, D. (2011). Effect of mixed corrosion inhibitors in cooling water system. Al-Khwarizmi Engineering Journal, 7(4), 76-87pag.
17. Shaban, A., Felhosi, I., & Vastag, G. (2017). Synergistic effect of sodium benzoate and EDTA as corrosion inhibitors for carbon steel in chloride-containing solutions. Corrosion Science, 125, 61–69. https://doi.org/10.1016/j.corsci.2017.06.027.

18. Brixi, N., Sail, L., Bezzar, A., Sebouai, O., & Benmesmoudi, S. (2018). Temperature effects on corrosion inhibition of mild steel in 3% NaCl solution by EDTA and sodium benzoate. In Proceedings of the Third International Symposium on Materials and Sustainable Development (pp. 385–397). Springer. https://doi.org/10.1007/978-3-319-89707-3_45
19. Ahmed, S. A., Kareem, S. B. A., & Makki, H. F. (2020, March). Investigation hydraulic performance of splash fills packing in cooling tower. AIP Conference Proceedings, 2213(1), 1–6. AIP Publishing. https://doi.org/10.1063/5.0000342
20. Handi, S. O., Jehawi, O. H., Dabah, A. M., & Odan, A. M. (2022). Synergy effect of corrosion inhibitors for protection of mild steel in cooling water system. International Science and Technology Journal, 13(31).
21. Arief, H., Pramudita, M., & Pitaloka, A. B. (2023). Synergistic ability of tannin–silica as a corrosion inhibitor with the addition of KI to mild steel in demineralized water. World Chemical Engineering Journal, 7(1), 11–17. https://doi.org/10.32734/wcej.v7i1.10067